

Fault Classification and Phase Selection Using Sequential Components

Athira Rajan¹, Jisha James²

PG Student [Power System], Dept. of EEE, Saintgits College of Engineering, Kottayam, Kerala, India,

Email: athiracem@gmail.com, Contact no:9497325836¹

Assistant professor, Dept. of EEE, Saintgits College of Engineering, Kottayam, Kerala, India²

Abstract— A new steady state based fault classification and faulted phase selection technique is proposed using the symmetrical components of reactive power. After extracting the symmetrical components of voltage current from sending end and receiving end the symmetrical components of reactive power are calculated. Based on these values we can classify single phase to ground, double phase and double phase to ground fault and also to select the faulted phase. The proposed method is a setting-free method because it does not need any threshold to operate. The simulation studies of different fault cases reveal the capability of the proposed method.

Keywords— Symmetrical Components, Fault classification, Faulted phase selection, Single phase to ground fault, Double phase fault, Double phase to ground fault.

INTRODUCTION

In power systems, protective devices detect fault conditions and operate circuit breakers and other devices to limit the loss of service due to a failure. Fast and reliable fault detection and fault classification technique is an important requirement in power transmission systems to maintain continuous power flow. Identifying the type of fault, e.g., single-phase grounding fault, phase-to-phase fault, etc. will help the relay to select different algorithm elements to deal with different fault situations. Identifying the faulted-phase helps to satisfy single-pole tripping and auto reclosing requirements and it becomes possible to only disconnect the faulted phase(s). This will increase the stability margin of the power system and probably avoid unnecessary loss of electricity in some regions.

A new steady-state-based approach to fault classification and faulted phase selection for single-circuit transmission lines is proposed by using the sequential reactive power components. Using the symmetrical components of voltage and current symmetrical reactive power components are calculated. Based on these values single phase to earth fault, phase to phase fault and double phase to earth fault can be identified. Also the faulted phase can be selected by analyzing the sequential reactive power components.

PROPOSED METHOD

The symmetrical components of reactive power are given by

$$Q_1 = \text{Im}\{V_1 * I_1^*\} \rightarrow (1)$$

$$Q_2 = \text{Im}\{V_2 * I_2^*\} \rightarrow (2)$$

$$Q_0 = \text{Im}\{V_0 * I_0^*\} \rightarrow (3)$$

where Q_1 , Q_2 , and Q_0 are, respectively, called positive-, negative-, and zero-sequence component of reactive power. Also, V_1 , V_2 , and V_0 are, respectively, positive-, negative-, and zero-sequence component of voltage measured at relay point (either sending or receiving end of Fig.1). Similarly, I_1 , I_2 , and I_0 are, respectively, positive-, negative-, and zero-sequence component of current measured at relay point. In this work, Q_2 and Q_0 will be utilized to develop the proposed method.



Fig. 1. Single-circuit transmission line protected by sending and receiving end relays.

A. Fault classification and faulted phase selection

- Single phase to ground fault

If the ratio Q_0/Q_2 is greater than 1 in any of the relay then it is a single phase to ground fault. $|Q_{20}|$ will have maximum value in the faulted phase.

- Double phase to ground fault

If the ratio Q_0/Q_2 is between 0 and 1 for both relays it is double phase to ground fault. For ABG fault $|Q_{20}|$ is maximum in phase C. If $|Q_{20}|$ is maximum in phase A it is BCG fault. For CAG fault $|Q_{20}|$ is maximum in phase B.

- Phase to phase fault

ΔQ_{12} is zero in healthy phase and non-zero for the faulty phase. Q_{12} is given by

$$Q_{12} = \text{Im}\{(V_1 + V_2) * (I_1 + I_2)^*\} \rightarrow (4)$$

B. Logical Pattern

Fig. 2 illustrates a flowchart of the proposed method in a logical pattern. Three phase currents and three phase voltages are sampled. Sequential reactive powers are calculated by using the sequential components of voltage and current. In Fig. 3, Q_{0S} and Q_{0R} stand for zero-sequence reactive power at sending and receiving ends, respectively. Similar definition holds for Q_{2S} and Q_{2R} .

After a fault inception is declared, the relays will firstly check if ΔQ_{12} is zero on one phase to identify phase-to-phase faults and to find the healthy phase. At this stage, the relays can either share their information or decide individually. If ΔQ_{12} not equal to zero on all three phases, ratio Q_0/Q_2 will be examined. From the view point of both relays, if $0 < Q_0/Q_2 < 1$, a double-phase-to-earth fault will be declared and if $Q_0/Q_2 > 1$ from the view point of at least one relay, a single-phase-to-earth fault will be declared. Here, both relays should share their own measurement by a pilot scheme. Faulted phase selection, however, is done locally, that is, each relay selects the faulted phase(s) by using its own measurement $|Q_{20}|$ as previously outlined.

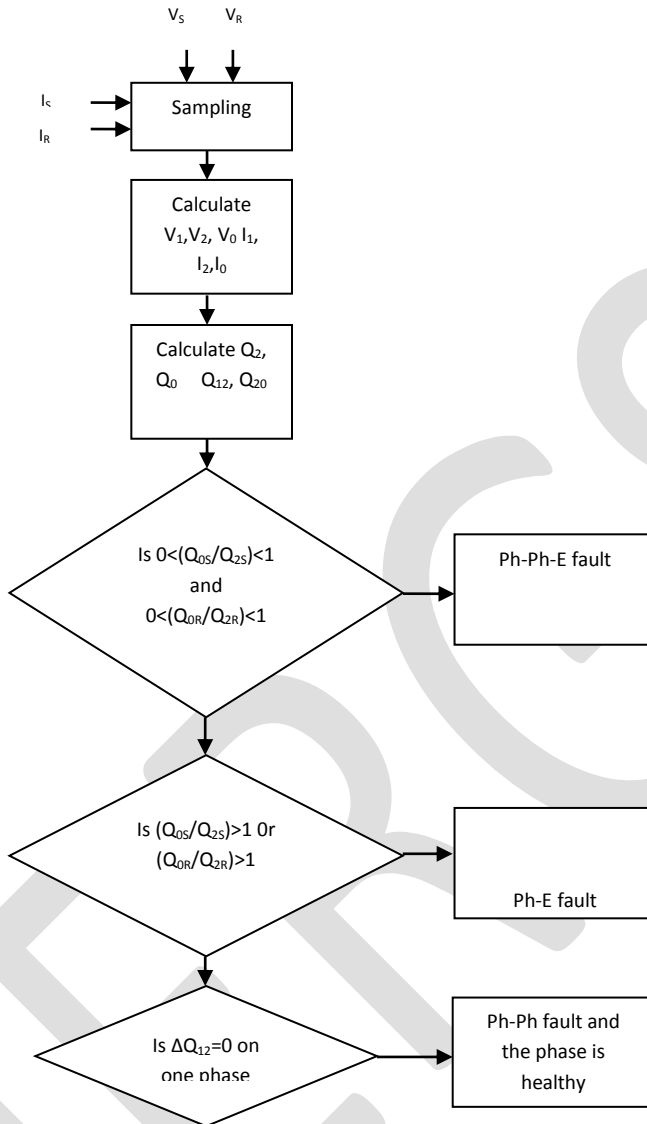


Fig. 2. Proposed method in a logical pattern.

RESULT AND DISCUSSION

The transmission line model is implemented in the PSCAD 4.2.1 professional version. The 50-Hz, 400-kV simulated system is shown in Fig. 3.

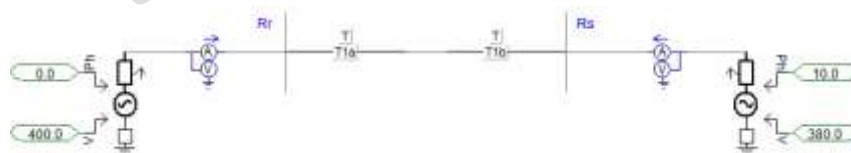


Fig. 3. PSCAD model of transmission line

The length of the transmission line was chosen 200 km. Sending end and receiving end sources are implemented using three phase voltage source model with base voltage level of 400kV and 380kV. The phase angles are set at 0° and 10° for sending end and receiving end respectively.

The fault classification and faulted phase selection algorithm was implemented using the MATLAB program. Various fault cases have been considered as tabulated in different tables. To avoid large numbers, Q_{20} and ΔQ_{12} are given in per unit (pu) with the base power of 100 MW.

Table I: Values measured by sending end for different single line to ground faults

Sl No.	Fault type	Fault resistance (Ω)	Fault distance (km)	Q_0/Q_2	$ Q_{20}^A $ (pu)	$ Q_{20}^B $ (pu)	$ Q_{20}^C $ (pu)
1	AG	10	10	1.6116	5.2957	1.1380	1.5655
2	AG	10	100	1.3742	0.4361	0.0913	0.1259
3	AG	10	190	0.4564	0.1022	0.0265	0.0288
4	BG	50	10	1.6116	0.1533	0.5189	0.1114
5	BG	50	100	1.3742	0.0346	0.1201	0.0251
6	BG	50	190	0.4564	0.0032	0.0114	0.0029
7	CG	100	10	1.6116	0.0299	0.0412	0.1394
8	CG	100	100	1.3742	0.0083	0.0114	0.0396
9	CG	100	190	0.4564	0.0008	0.0008	0.0031

Table II: Values measured by receiving end for different single line to ground faults

Sl No.	Fault type	Fault resistance (Ω)	Fault distance (km)	Q_0/Q_2	$ Q_{20}^A $ (pu)	$ Q_{20}^B $ (pu)	$ Q_{20}^C $ (pu)
1	AG	10	190	0.4987	0.1622	0.0305	0.1197
2	AG	10	100	1.4010	0.5199	0.1152	0.1501
3	AG	10	10	1.5895	5.2787	1.1968	1.1354
4	BG	50	190	0.4987	0.0033	0.0117	0.0131
5	BG	50	100	1.4010	0.0403	0.1431	0.0319
6	BG	50	10	1.5895	0.1684	0.5885	0.1260
7	CG	100	190	0.4987	0.0008	0.0008	0.0125
8	CG	100	100	1.4010	0.0104	0.0133	0.0487

9	CG	100	10	1.5895	0.0363	0.1058	0.1002
---	----	-----	----	--------	--------	--------	--------

As Tables I and II show, the ratio of Q_0/Q_2 was more than 1 at either one end or both ends in case of single-phase-to-earth faults. This confirmed a single-phase-to-earth fault inception. For the AG faults, the maximum $|Q_{20}|$ occurred on Phase A. For BG and CG faults, maximum $|Q_{20}|$ occurred on Phases B and C, respectively. Therefore, the faulted phase was selected. It is clear that the method can cope with high fault resistance and any fault location.

Table III: Values measured by sending end for different double line to ground faults

Sl No.	Fault type	Fault resistance (Ω)	Fault distance (km)	Q_0/Q_2	$ Q_{20}^A $ (pu)	$ Q_{20}^B $ (pu)	$ Q_{20}^C $ (pu)
1	ABG	10	10	0.6290	0.9808	2.2587	6.1416
2	ABG	10	100	0.1852	0.2261	0.3239	0.7478
3	ABG	10	190	0.1821	0.0425	0.0580	0.1364
4	ACG	50	30	0.9479	0.1646	0.3986	0.0463
5	ACG	50	100	0.5769	0.0631	0.1346	0.0148
6	ACG	50	175	0.5293	0.0089	0.0225	0.0035
7	BCG	100	70	0.9947	0.0656	0.0079	0.0264
8	BCG	100	100	0.8991	0.0412	0.0048	0.0169
9	BCG	100	130	0.8396	0.0233	0.0019	0.0093

Table IV: Values measured by receiving end for different double line to ground faults

Sl No.	Fault type	Fault resistance (Ω)	Fault distance (km)	Q_0/Q_2	$ Q_{20}^A $ (pu)	$ Q_{20}^B $ (pu)	$ Q_{20}^C $ (pu)
1	ABG	10	190	0.1946	0.0476	0.0685	0.7118
2	ABG	10	100	0.1888	0.2740	0.3768	0.9303
3	ABG	10	10	0.6343	1.0867	2.1257	3.2993
4	ACG	50	170	0.6020	0.0123	0.0308	0.0125
5	ACG	50	100	0.5881	0.0734	0.1607	0.0199
6	ACG	50	25	0.9931	0.1916	0.4919	0.0576
7	BCG	100	130	0.8773	0.0278	0.0037	0.0154
8	BCG	100	100	0.9167	0.0492	0.0063	0.0203

9	BCG	100	70	0.9910	0.0779	0.0105	0.0248
---	-----	-----	----	--------	--------	--------	--------

For double-phase-to-earth faults, Q_0/Q_2 was less than 1 at both ends, as seen in Tables III and IV. This confirmed a double-phase-to-earth fault. For ABG faults, $|Q_{20}|$ was the maximum on Phase C. For BCG and CAG faults, was the maximum on Phases A and B respectively. This disclosed the faulted phases. But the fault classification technique fails when fault location is on the extreme ends of the transmission line for high fault resistance case. As the fault resistance increases the span of length of transmission line in which the proposed method works reduces.

Table V and VI presents ΔQ_{12} on each phase measured by relays R_S and R_R for different phase-to-phase fault cases as tabulated, ΔQ_{12} were nearly zero on the healthy phase while they were not zero on the faulted phases.

Table V: Values measured by sending end for different phase to phase faults

Sl No.	Fault type	Fault resistance (Ω)	Fault distance (km)	$ \Delta Q_{12}^A $ (pu)	$ \Delta Q_{12}^B $ (pu)	$ \Delta Q_{12}^C $ (pu)
1	AB	10	20	3.4504	19.3470	0.0009
2	AB	10	100	5.6532	10.3340	0.00006
3	AB	10	180	2.5493	6.3656	0.0006
4	AC	50	20	8.4356	0.0009	4.3539
5	AC	50	100	5.7786	0.00005	0.5113
6	AC	50	180	2.2233	0.0007	0.8158
7	BC	100	20	0.0009	3.0066	4.1922
8	BC	100	100	0.00004	1.2527	2.8809
9	BC	100	180	0.0007	0.7324	0.9828

Table VI: Values measured by receiving end for different phase to phase faults

Sl No.	Fault type	Fault resistance (Ω)	Fault distance (km)	$ \Delta Q_{12}^A $ (pu)	$ \Delta Q_{12}^B $ (pu)	$ \Delta Q_{12}^C $ (pu)
1	AB	10	180	3.1383	5.8105	0.0013
2	AB	10	100	5.5453	8.7675	0.00005
3	AB	10	20	2.0256	14.1510	0.0010
4	AC	50	180	2.1911	0.0013	0.2853

5	AC	50	100	5.4187	0.00007	0.0270
6	AC	50	20	7.2563	0.0010	3.9583
7	BC	100	180	0.0013	0.3789	1.0404
8	BC	100	100	0.00004	0.8215	2.8416
9	BC	100	20	0.0010	2.7709	3.7155

CONCLUSION

A new fault classification and faulted phase selection technique in single-circuit transmission by using the symmetrical components of electrical quantities lines was proposed. It is setting-free since it works with constant thresholds, that is, 1 and 0. Since setting these functions always requires struggles this feature of protective functions is very attractive. Another advantage is that it utilizes Q_0/Q_2 at each end and, thus, data of each end are not required to be synchronized since Q_0 and Q_2 are scalar quantities. This eliminates any concern about data synchronization. Moreover, the proposed method will not act on any symmetrical conditions which resemble faults, such as power swings and overloading since only zero-sequence and negative-sequence reactive power are used. The simulation results show that the capability of the system with high fault resistance.

But the fault classification technique for double phase to earth fault fails when fault location is on the extreme ends of the transmission line for high fault resistance case. As the fault resistance increases the span of length of transmission line in which the proposed method works reduces. Future work will expand to resolve this problem.

REFERENCES:

- [1] A. Jamehbozorg and S. M. Shahrtash, "A decision-tree-based method for fault classification in single-circuit transmission lines," *IEEE Trans. Power Del.*, vol. 25, no. 4, pp. 2190–2196, Oct. 2010.
- [2] O. A. S. Youssef, "New algorithm to phase selection based on wavelet transforms," *IEEE Trans. Power Del.*, vol. 17, no. 4, pp. 908–914, Oct. 2002.
- [3] Z. He, L. Fu, S. Lin, and Z. Bo, "Fault detection and classification in EHV transmission line based on wavelet singular entropy," *IEEE Trans. Power Del.*, vol. 25, no. 4, pp. 2156–2163, Oct. 2010.
- [4] X. Dong, W. Kong, and T. Cui, "Fault classification and faulted-phase selection based on the initial current traveling wave," *IEEE Trans. Power Del.*, vol. 24, no. 2, pp. 552–559, Apr. 2009.
- [5] G. Benmouyal and J. Mahseredjian, "A combined directional and faulted phase selector element based on incremental quantities," *IEEE Trans. Power Del.*, vol. 16, no. 4, pp. 478–484, Oct. 2001.
- [6] T. Adu, "An accurate fault classification technique for power system monitoring devices," *IEEE Trans. Power Del.*, vol. 17, no. 3, pp. 684–690, Jul. 2002.
- [7] X.-N. Lin, M. Zhao, K. Alymann, and P. Liu, "Novel design of a fast phase selector using correlation analysis," *IEEE Trans. Power Del.*, vol. 20, no. 2, pt. 2, pp. 1283–1290, Apr. 2005.
- [8] P. K. Dash, S. R. Samantaray, and G. Panda, "Fault classification and section identification of an advanced series compensated transmission line using support vector machine," *IEEE Trans. Power Del.*, vol. 22, no. 1, pp. 67–73, Jan. 2007.
- [9] R. Salat and S. Osowski, "Accurate fault location in the power transmission line using support vector machine approach," *IEEE Trans. Power Syst.*, vol. 29, no. 2, pp. 979–986, May 2004.
- [10] Wang and W. W. L. Keerthipala, "Fuzzy-neuro approach to fault classification for transmission line protection," *IEEE Trans. Power Del.*, vol. 13, no. 4, pp. 1093–1104, Oct. 1998.
- [11] Behnam Mahamedi and Jian Guo Zhu, "Fault Classification and Faulted Phase Selection Based on the Symmetrical Components of Reactive Power for Single-Circuit Transmission Lines," *IEEE Trans. Power Del.*, vol. 28, no. 4, October 2013.

- [12] Abouzar Rahmati and Reza Adhami, "A Fault Detection and Classification Technique Based on Sequential Components,"
IEEE Trans. Industry Applications, vol. 50, no. 6, December 2014

IJERGS